

Dipole anisotropy and identification of UHECR sources

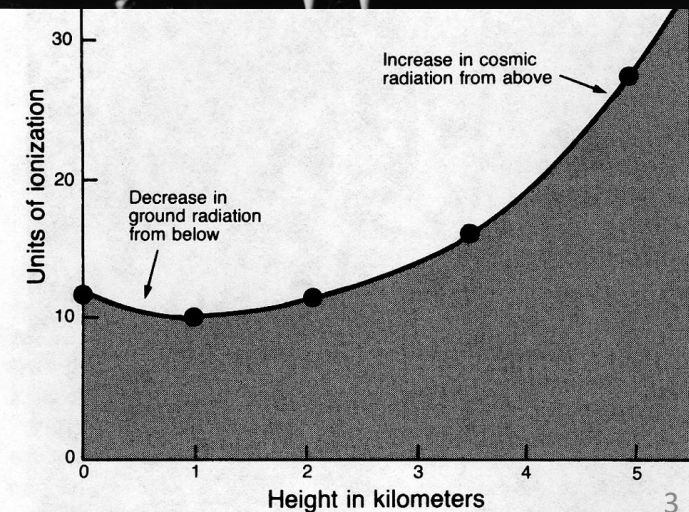
Outlook

1. History
2. Propagation of cosmic rays in the universe
3. Galactic Magnetic Field
4. Large scale dipole anisotropy in arrival directions
5. Deflections of cosmic rays from strong nearby sources
6. Conclusions and plans

History

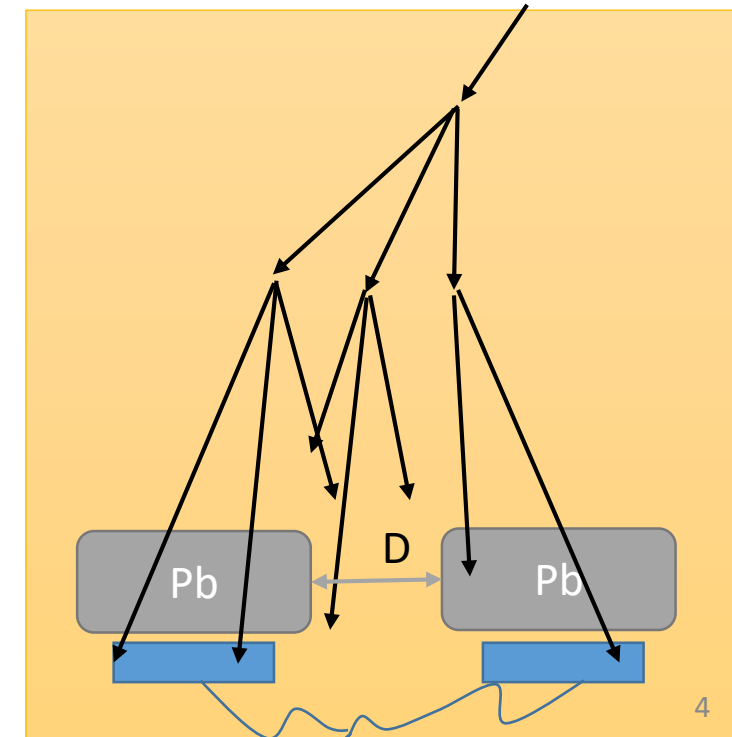
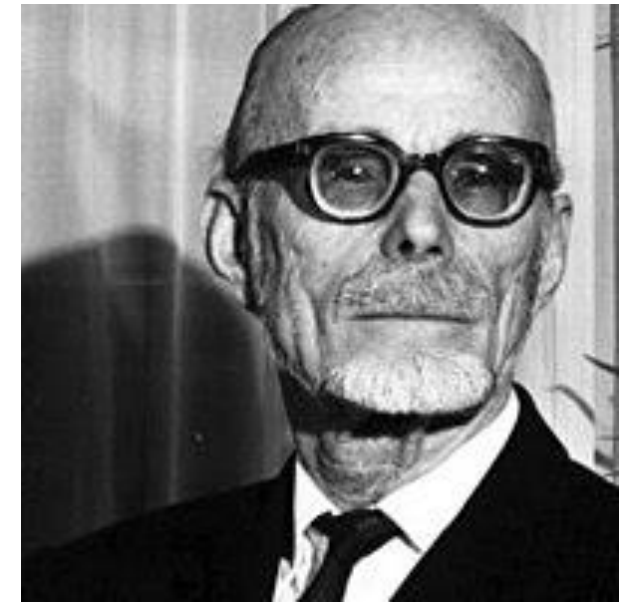
- 1911-1912 Victor Franz Hess – balloon flights and measurement of ionization in different altitudes
 - Hypothesis: radiation causing the ionization comes from Earth
 - Measured data indicate an increasing radiation with altitude
 - CONCLUSION: radiation originates in space → DISCOVERY OF COSMIC RAYS (1936 Nobel prize)

"The results of the observations indicate that rays of very great penetrating power are entering our atmosphere from above. "



History

- 1930' – known cosmic rays with energies up to 10 GeV
- 1938 – maximum energy of cosmic rays increases by 5 orders of magnitude
- 1938 - *Pierre Victor Auger* discovers extended air showers of secondary cosmic rays
 - Experiment in Swiss Alps, individual detectors placed up to 300 m from each other – looking for coincidental signals
 - Estimated energy of primary cosmic-ray particle 10^{15} eV



History

- 1959 – John Linsley and Livio Scarsi build first detector array with area 1 km² in Volcano Ranch, New Mexico
- First measurement of energy spectrum of cosmic rays above 10¹⁸ eV
- 1962 – Linsley detects a first event with energy of the primary cosmic ray exceeding 10²⁰ eV

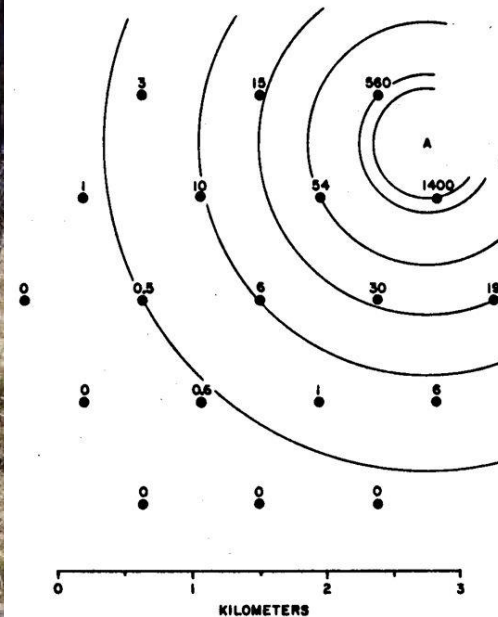


FIG. 1. Plan of the Volcano Ranch array in February

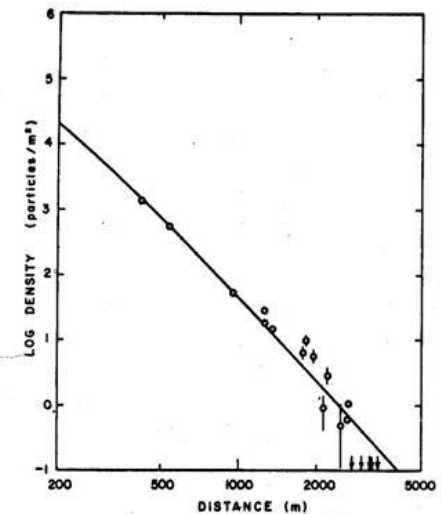
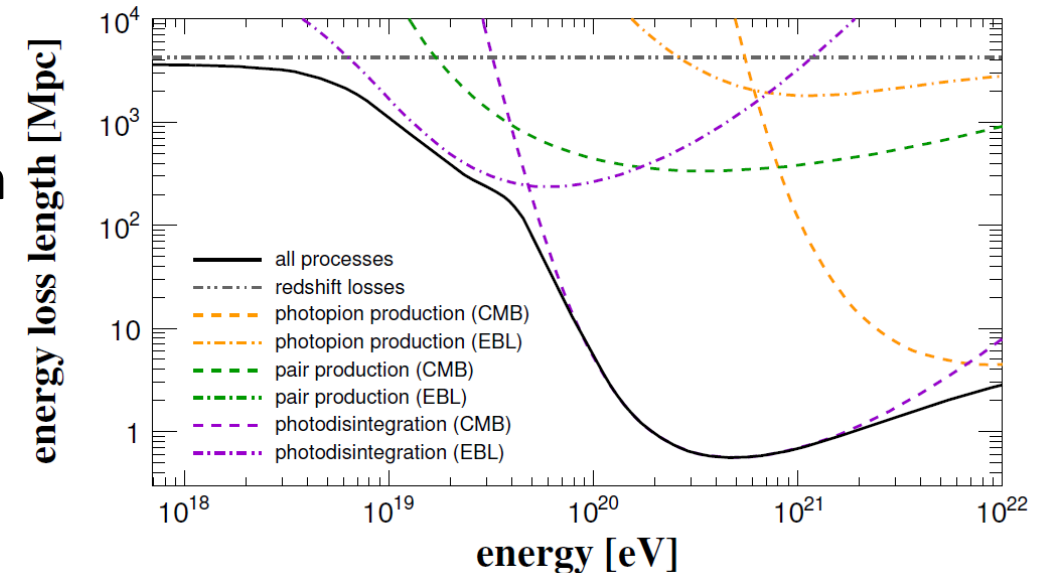


FIG. 2. Observed shower densities as a function of distance from the shower axis. The curve is the Greisen approximation of the Nishimura-Kamata lateral distribution for $s = 1.0$, $N = 5 \times 10^{19}$.

Propagation of cosmic rays in the universe

- Interactions with photon fields (CMB, EBL)
- Energy losses and change of composition
- Large mean free paths \rightarrow negligible for propagation inside our Galaxy
- Charged particles – deflection in magnetic fields
- Deflections depend on strength of the magnetic field and **rigidity** of the particle

$$R = \frac{E}{Z}$$



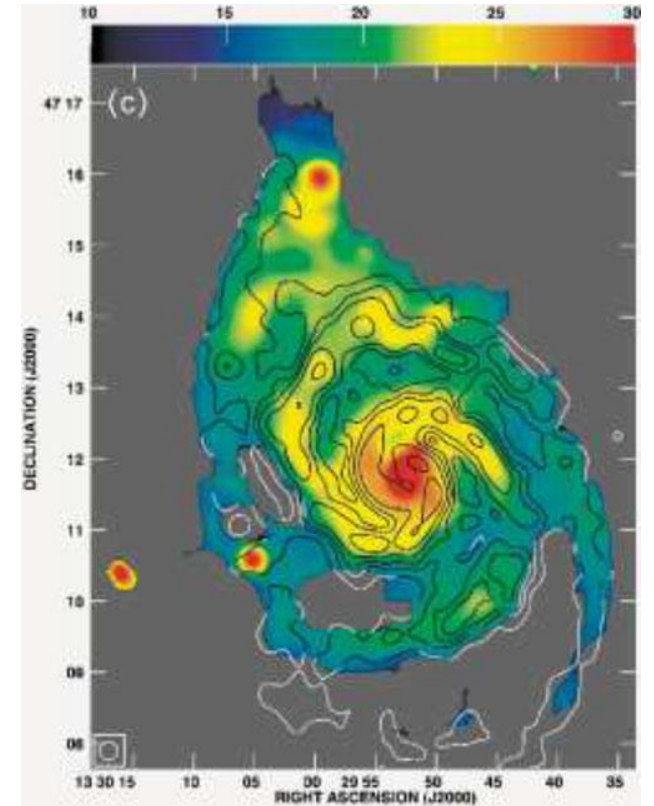
Magnetic fields in the Universe

Galactic magnetic field

- Dynamo – motion of turbulent gas generates a large-scale regular field
- Typical strength for spiral galaxies is about $10 \mu\text{G}$
- Milky Way - about $6 \mu\text{G}$ near the Sun, increases to $(20-40) \mu\text{G}$ in the Galactic center region
- Large-scale regular field is mostly parallel to the plane of the Galactic disk

Extragalactic magnetic fields

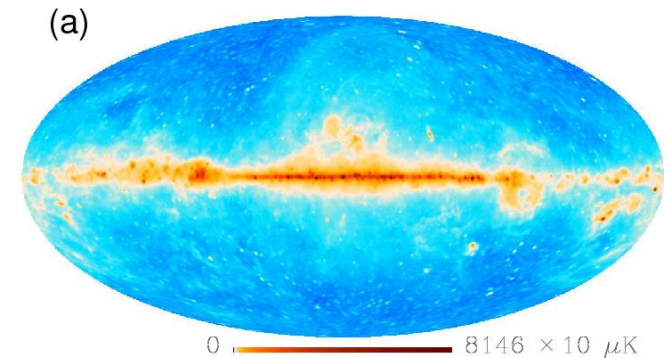
- Weak in comparison with GMF ($< \text{nG}$)



How to Measure the Strength of Magnetic Fields?

Synchrotron radiation

- Emitted by electrons, intensity is sensitive to magnetic field strength
- Degree of polarization about 75%, observed polarization is lower due to contamination by unpolarized thermal emission



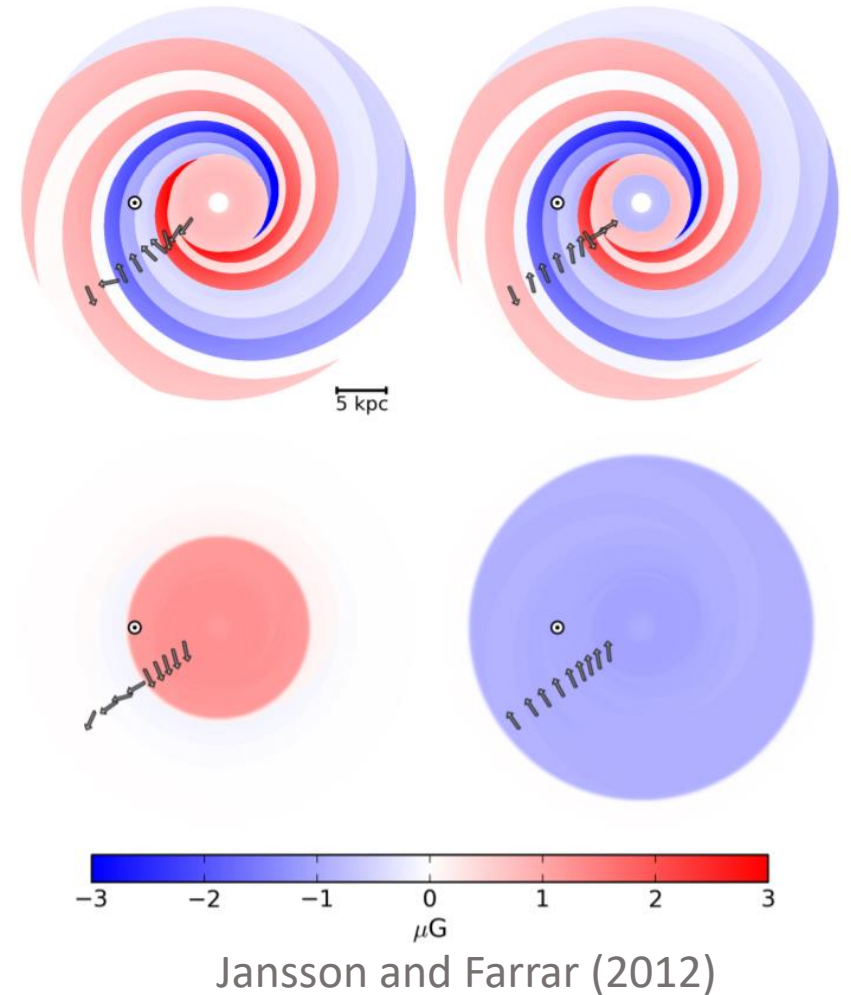
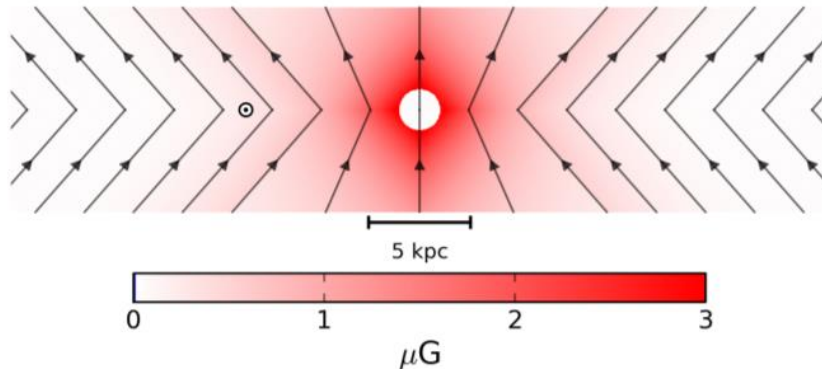
Faraday rotation measures

- Faraday rotation = change of line of polarization when travelling through magnetic field
- Rotation angle is sensitive to the sign of the field direction
- Used for measurements of regular magnetic fields

Zeeman splitting, polarized optical light ...

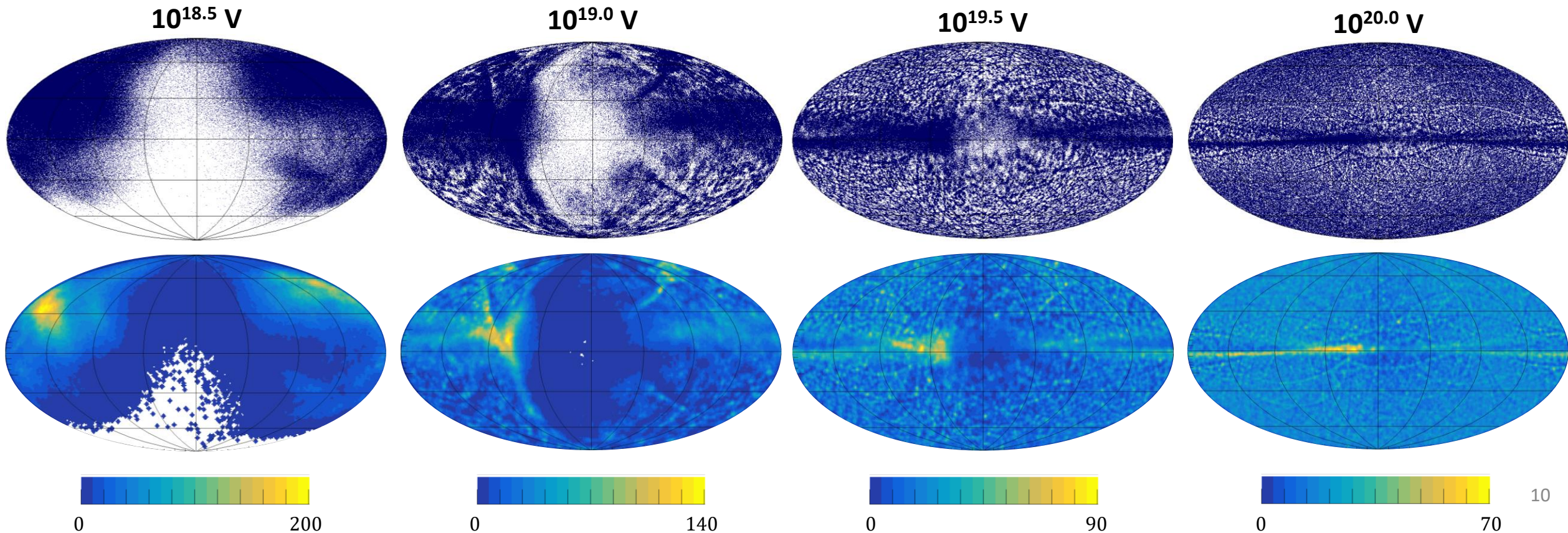
Galactic Magnetic Field – JF12

- Jansson and Farrar model
- Used data from both faraday rotation measures and polarized synchrotron radiation
- Disk field and an extended halo field
- Regular, turbulent and striated components of the GMF



Deflections in Galactic Magnetic Field

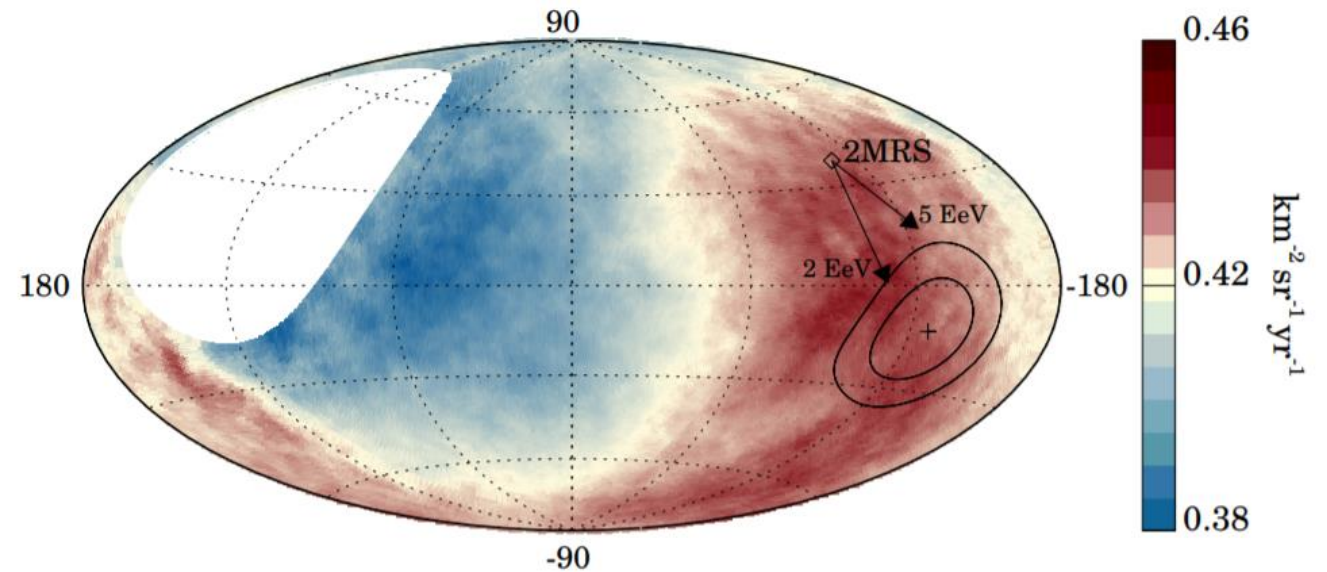
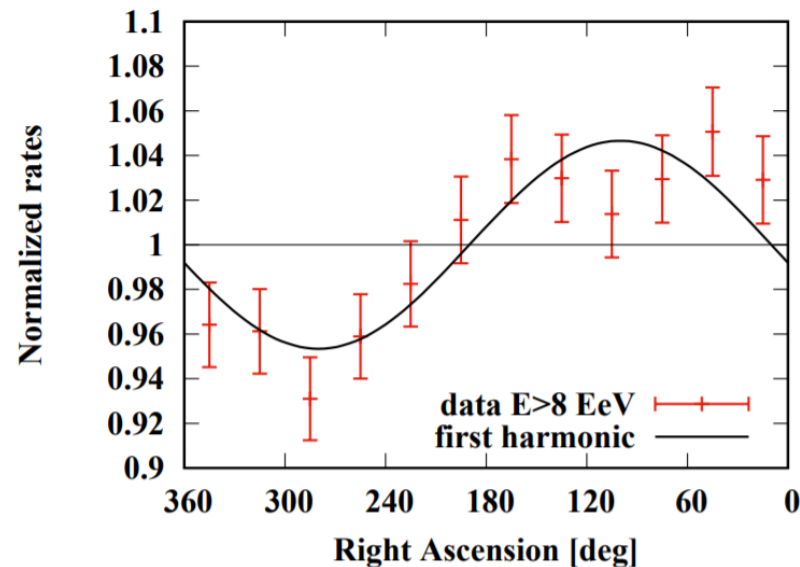
- Simulation: backtracking in JF12, isotropic flux from Earth propagated to the border of the Galaxy
- Existence of preferred directions, some sources are invisible at lower rigidities



Large Scale Dipole Anisotropy in Arrival Directions

Pierre Auger Observatory Measurement

- Dipole in arrival directions above 8 EeV with magnitude $\sim 6\%$
- Direction of the dipole: $(\alpha, \delta) = (98^\circ, -25^\circ)$
- Dipole points $\sim 125^\circ$ away from direction of galactic center

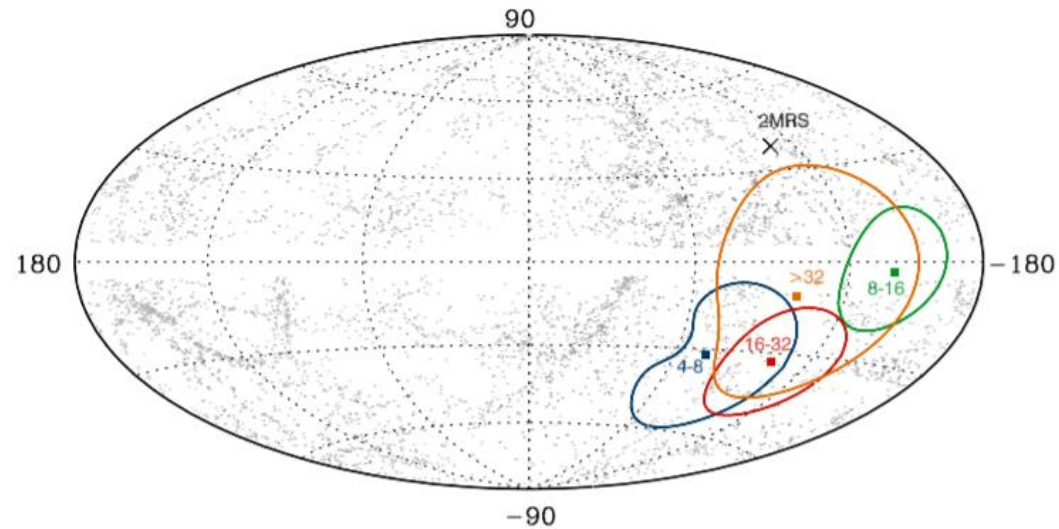
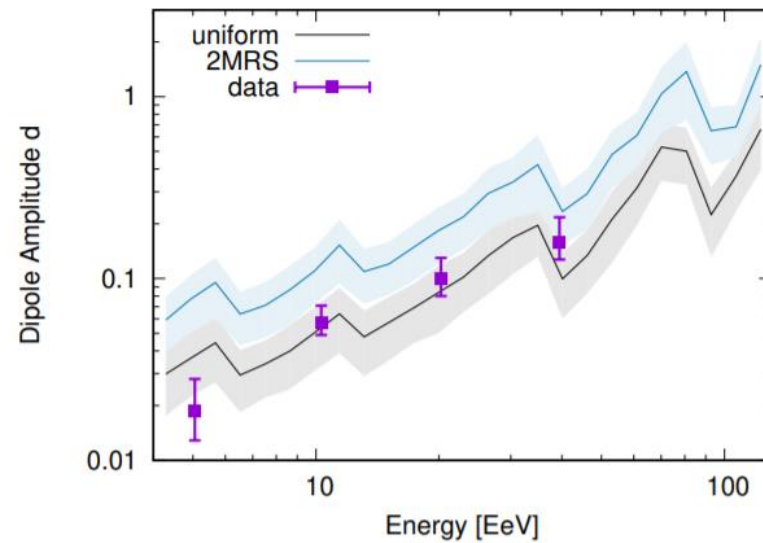


| Energy [EeV] | Number of events | Fourier coefficient a_α | Fourier coefficient b_α | Amplitude r_α | Phase φ_α [°] | Probability $P(\geq r_\alpha)$ |
|--------------|------------------|--------------------------------|--------------------------------|---------------------------|----------------------------|--------------------------------|
| 4 to 8 | 81,701 | 0.001 ± 0.005 | 0.005 ± 0.005 | $0.005^{+0.006}_{-0.002}$ | 80 ± 60 | 0.60 |
| ≥ 8 | 32,187 | -0.008 ± 0.008 | 0.046 ± 0.008 | $0.047^{+0.008}_{-0.007}$ | 100 ± 10 | 2.6×10^{-8} |

| Energy [EeV] | N | d_\perp | d_z | d | α_d [°] | δ_d [°] |
|--------------|--------|-----------|---------------------------|--------------------|---------------------------|----------------|
| interval | median | | | | | |
| 4 - 8 | 5.0 | 88,317 | $0.010^{+0.007}_{-0.004}$ | -0.016 ± 0.009 | $0.019^{+0.009}_{-0.006}$ | 70 ± 34 |
| ≥ 8 | 11.5 | 36,924 | $0.060^{+0.010}_{-0.009}$ | -0.028 ± 0.014 | $0.066^{+0.012}_{-0.008}$ | 98 ± 9 |

Pierre Auger Observatory Measurement

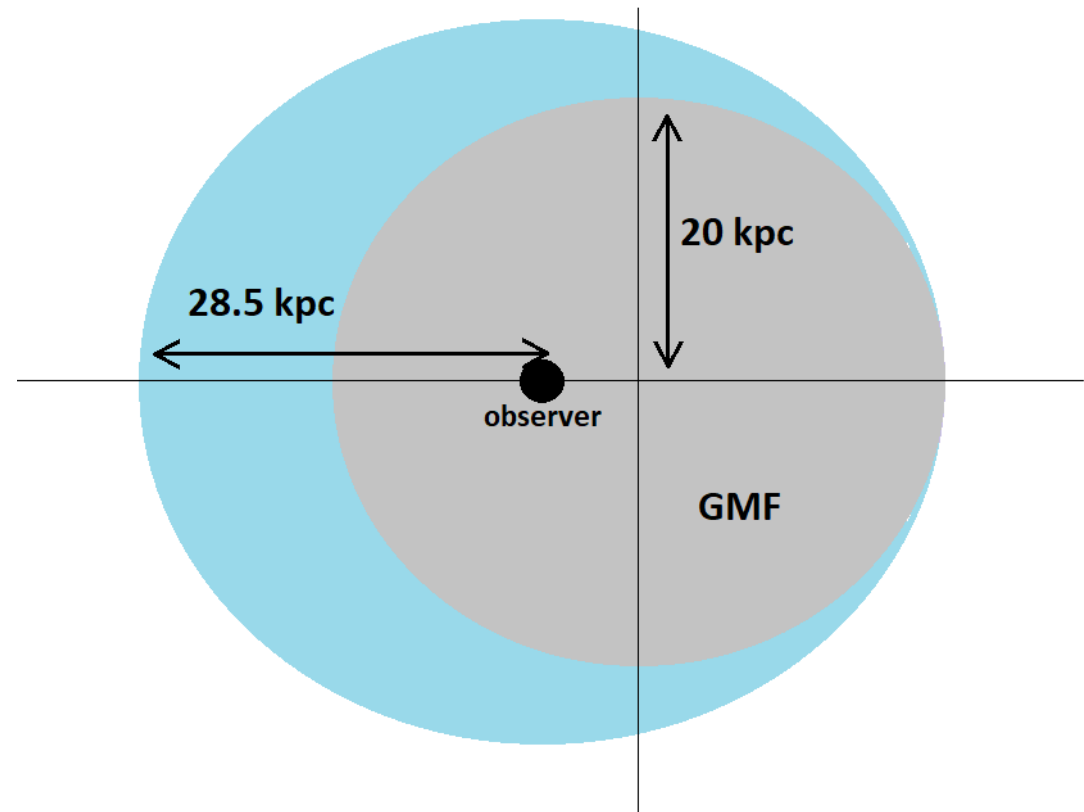
- Dipole amplitude increases with higher threshold energy, statistics goes down
- Of all energy intervals, ≥ 8 EeV has the highest significance



| Energy [EeV] | N | d_{\perp} | d_z | d | α_d [°] | δ_d [°] | |
|--------------|--------|-------------|---------------------------|--------------------|---------------------------|----------------|-------------------|
| interval | median | | | | | | |
| 4 - 8 | 5.0 | 88,325 | $0.010^{+0.007}_{-0.004}$ | -0.016 ± 0.009 | $0.019^{+0.009}_{-0.006}$ | 69 ± 46 | -57^{+24}_{-20} |
| ≥ 8 | 11.5 | 36,928 | $0.060^{+0.010}_{-0.009}$ | -0.028 ± 0.014 | $0.066^{+0.012}_{-0.008}$ | 98 ± 9 | -25 ± 11 |
| 8 - 16 | 10.3 | 27,271 | $0.056^{+0.012}_{-0.010}$ | -0.011 ± 0.016 | $0.057^{+0.014}_{-0.008}$ | 97 ± 12 | -11 ± 16 |
| 16 - 32 | 20.2 | 7,664 | $0.075^{+0.023}_{-0.018}$ | -0.07 ± 0.03 | $0.10^{+0.03}_{-0.02}$ | 80 ± 17 | -44 ± 14 |
| ≥ 32 | 39.5 | 1,993 | $0.13^{+0.05}_{-0.03}$ | -0.09 ± 0.06 | $0.16^{+0.06}_{-0.03}$ | 152 ± 19 | -34^{+19}_{-20} |

Simulations in CRPropa 3

- Simulations performed in CRPropa 3
- Isotropic flux to the galaxy
- Power law energy spectrum (8-100) EeV
- Direct simulations of p, He, N propagated in JF12 model of GMF
- Full JF12 GMF model – regular, striated and turbulent field
- Observer at position (-8.5,0,0) kpc with radius 100 pc
- Energy losses on CMB and EBL are neglected



Reconstruction of the Dipole

- Analysis in right ascension (RA) – uniform exposure
- Rayleigh analysis – fourier analysis in right ascension

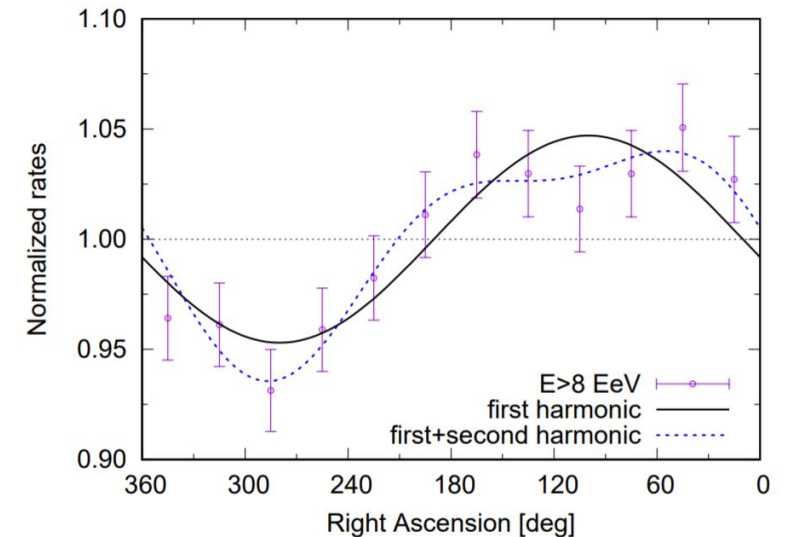
$$a_k = \frac{2}{N} \sum_i w_i \cos(k\alpha) \quad b_k = \frac{2}{N} \sum_i w_i \sin(k\alpha)$$

- **Amplitude** of the dipole in RA

$$r_k = \sqrt{a_k^2 + b_k^2}$$

- **Phase** of the dipole

$$\varphi_k = \frac{1}{k} \tan^{-1} \left(\frac{b_k}{a_k} \right)$$



Reconstruction of the Dipole

- Assumed shape of the CR angular distribution with dipole behavior with unit vector pointing in the direction of the dipole \mathbf{D} and amplitude α

$$\Phi(\mathbf{u}) = \frac{\Phi_0}{4\pi} (1 + \alpha \mathbf{D} \cdot \mathbf{u}) \quad (1)$$

- Zero and first moments of the flux

$$I_0 = \int \Phi(\mathbf{u}) d\Omega, \quad \mathbf{I} = \int \mathbf{u} \Phi(\mathbf{u}) d\Omega \quad (2)$$

- Using (1) and (2)

$$I_0 = \Phi_0, \quad \mathbf{I} = \frac{1}{3} \Phi_0 \times \alpha \mathbf{D} \quad (3)$$

- Working with finite amount of simulated data we need a discrete versions of these integrals

$$S_0 = \sum_k \frac{1}{\varepsilon_k}, \quad \mathbf{S} = \sum_k \frac{\mathbf{u}_k}{\varepsilon_k} \quad (4)$$

Reconstruction of the Dipole

$$S_0 = \sum_k \frac{1}{\varepsilon_k}, \quad \mathbf{S} = \sum_k \frac{\mathbf{u}_k}{\varepsilon_k}$$

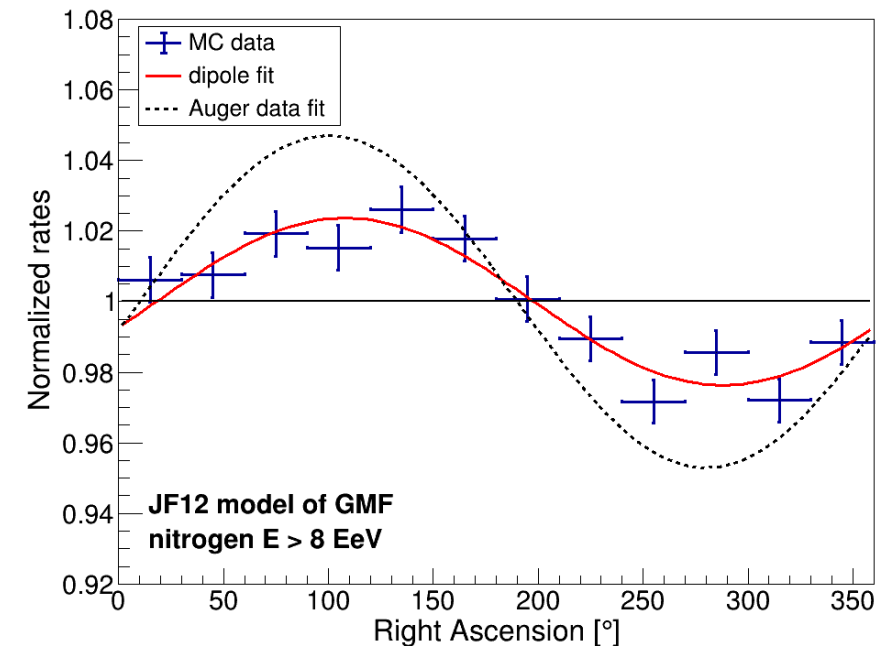
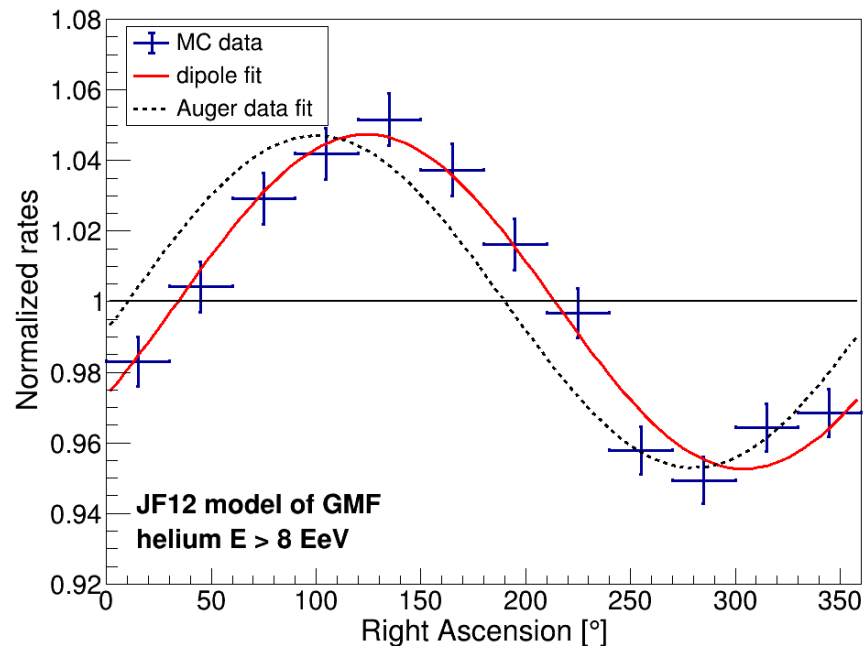
- Amplitude and direction of the dipole can be derived directly from the identification with I_0 and \mathbf{I}

$$\alpha = \frac{3\|\mathbf{S}\|}{S_0}, \quad \mathbf{D} = \frac{\mathbf{S}}{\|\mathbf{S}\|}$$

- More accurate when total number of events N is large

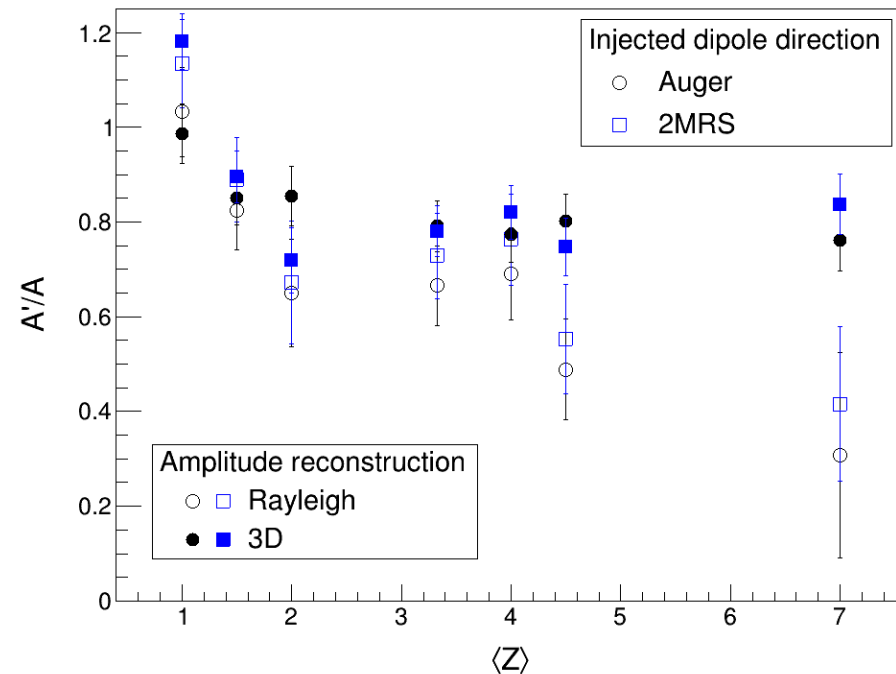
Injection of a dipole

- Simulated data reweighted by dipolar distribution in the direction of 2MRS $(l, b) = (251^\circ, 37^\circ)$
- Reconstruction of dipole in right ascension and 3D – amplitude and direction
- Rayleigh: only small changes of the phase, amplitude is strongly suppressed for lower rigidities



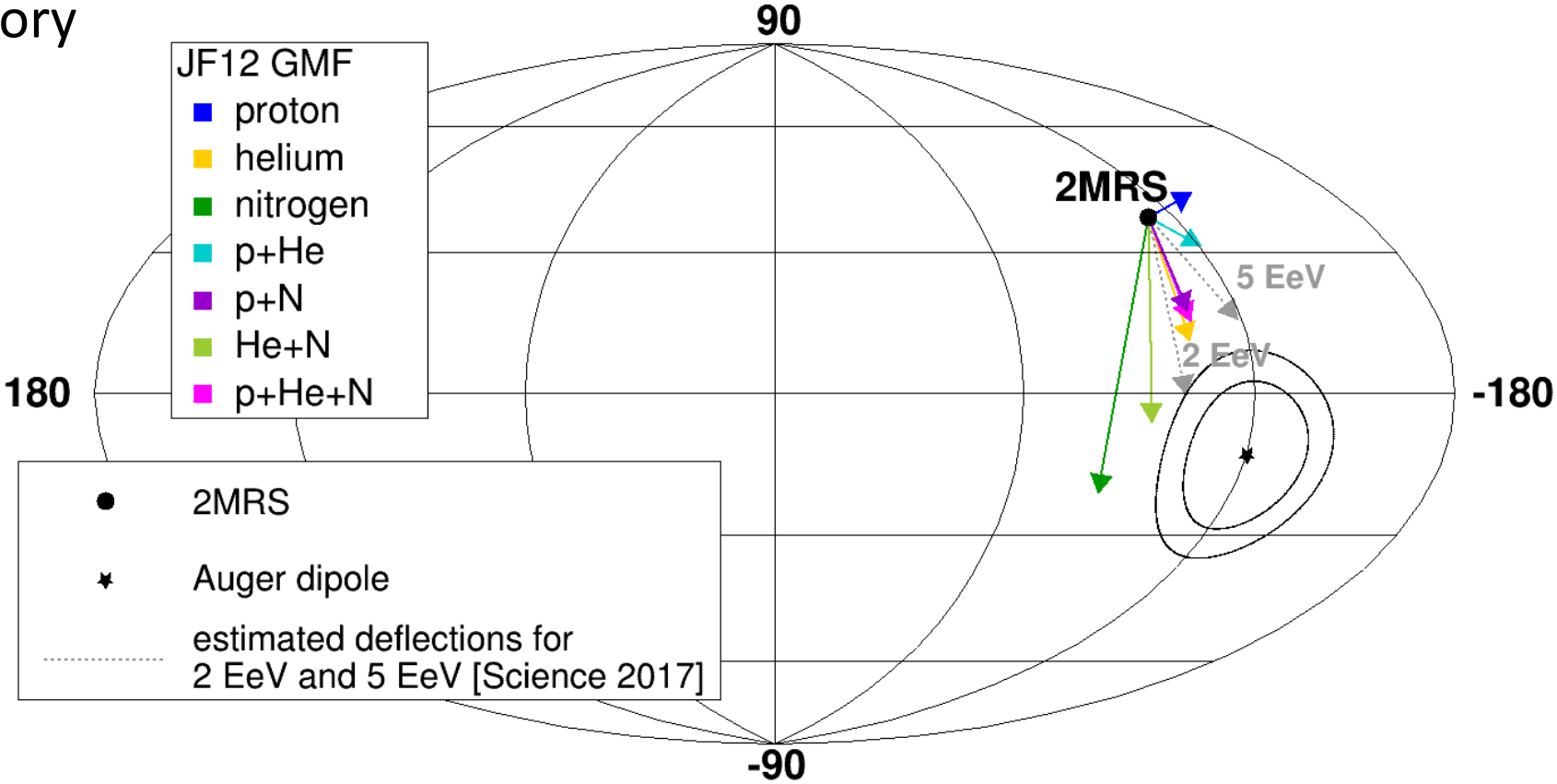
Reconstructed dipole – 2MRS dipole direction

- Relative change of the observed amplitude on the observer
- Amplitude decreases for heavier composition in case of dipole in right ascension down to $\sim 40\%$ of the injected amplitude
- Amplitude of the 3D dipole remains $\sim 80\%$ of the injected one even for pure N

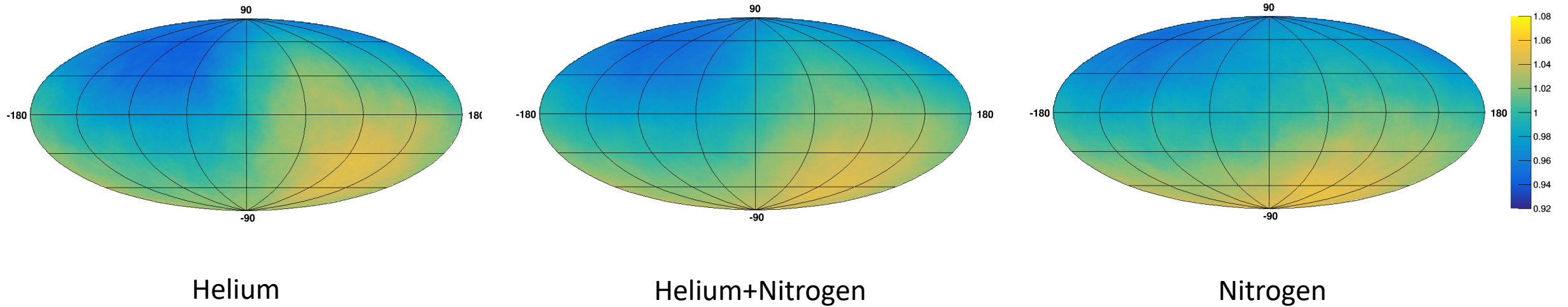


Reconstructed dipole – 2MRS dipole direction

- Direction of the dipole changes after propagation in GMF
- Heavier composition points close to the observed dipole direction by the Pierre Auger Observatory



Reconstructed dipole – 2MRS dipole direction



- Simulated data smoothed by 45° tophat
- Slight decrease of the dipole amplitude for heavier composition, change of the direction of the dipole

Deflections of cosmic rays from strong nearby sources

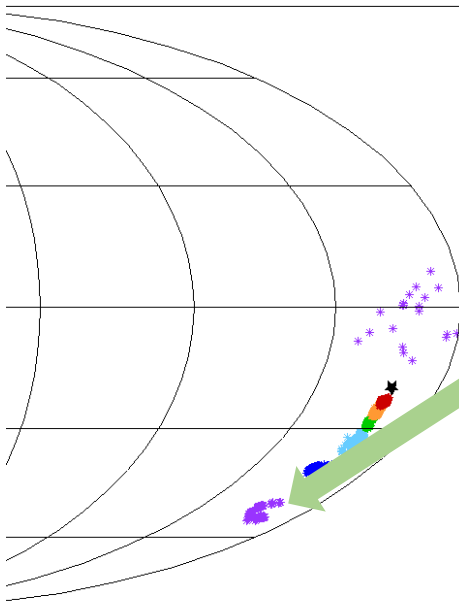
Simulations

- Simulation performed in CRPropa 3
- Antiprotons backtracked in the JF12 model of GMF
- Discrete energy $\log\left(\frac{E}{\text{eV}}\right) = (19.0 - 20.0)$ with a step 0.1

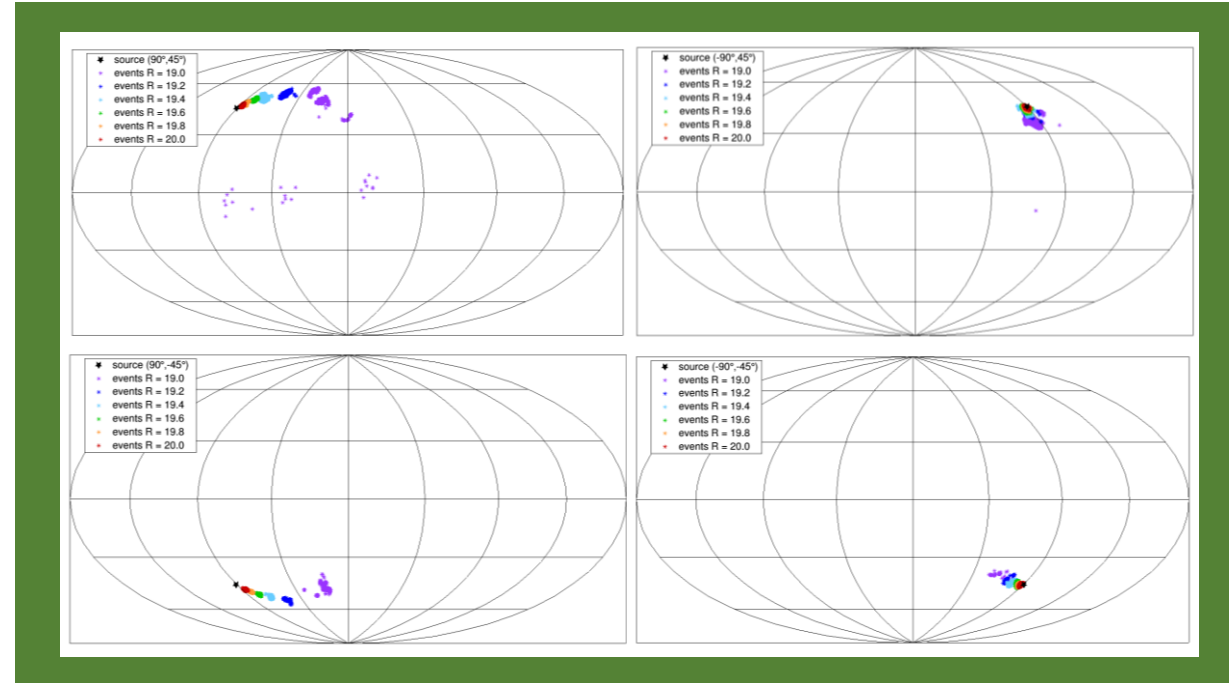
- 6 chosen sources within 70 Mpc from catalogue of closest strong radio sources
 - Centaurus A, Fornax A , Messier 87 , NGC4261 , UGC1841 , CGCG 114-025
- Simulated particles are assigned to given source if they point within 1° from its direction – partly covers deflections in EGMF and finite source size

Deflections in Galactic Magnetic Field

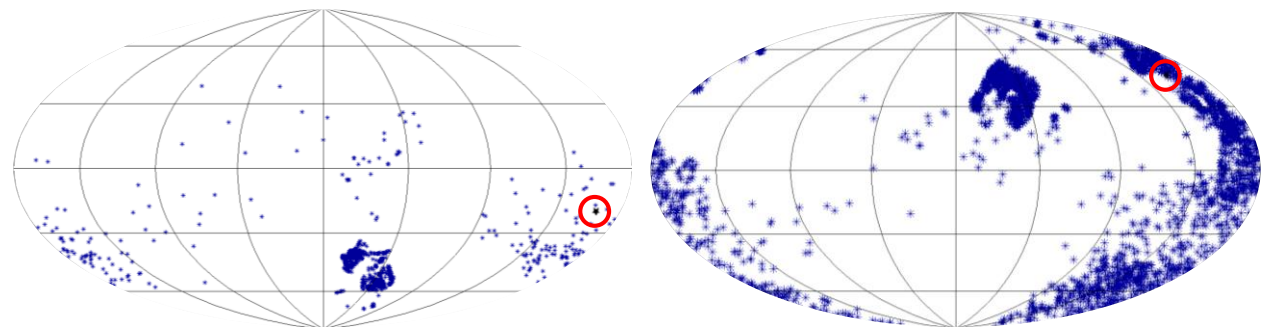
- No “simple recipe” to where events from a source will display on the sky
- Strongly depends on position of the source and rigidity
- For lower rigidities deflections even tens of degrees



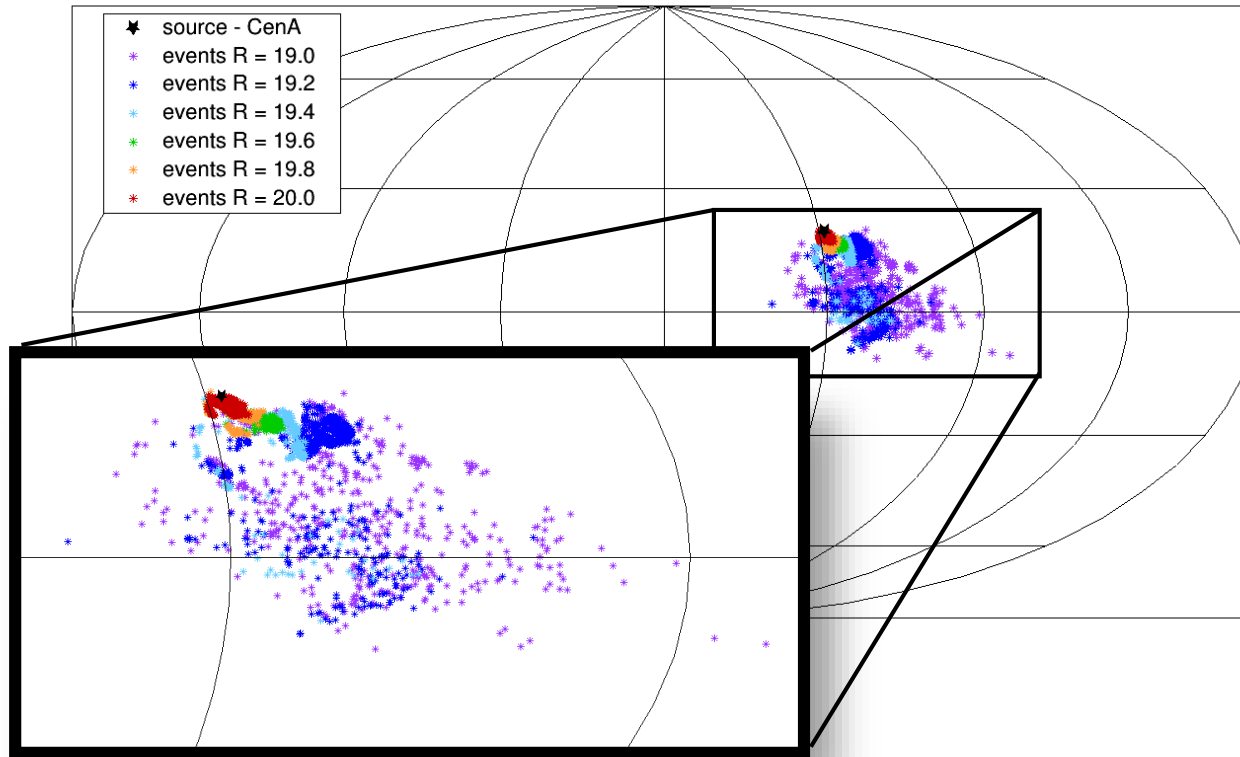
Multiple imaging
of a source



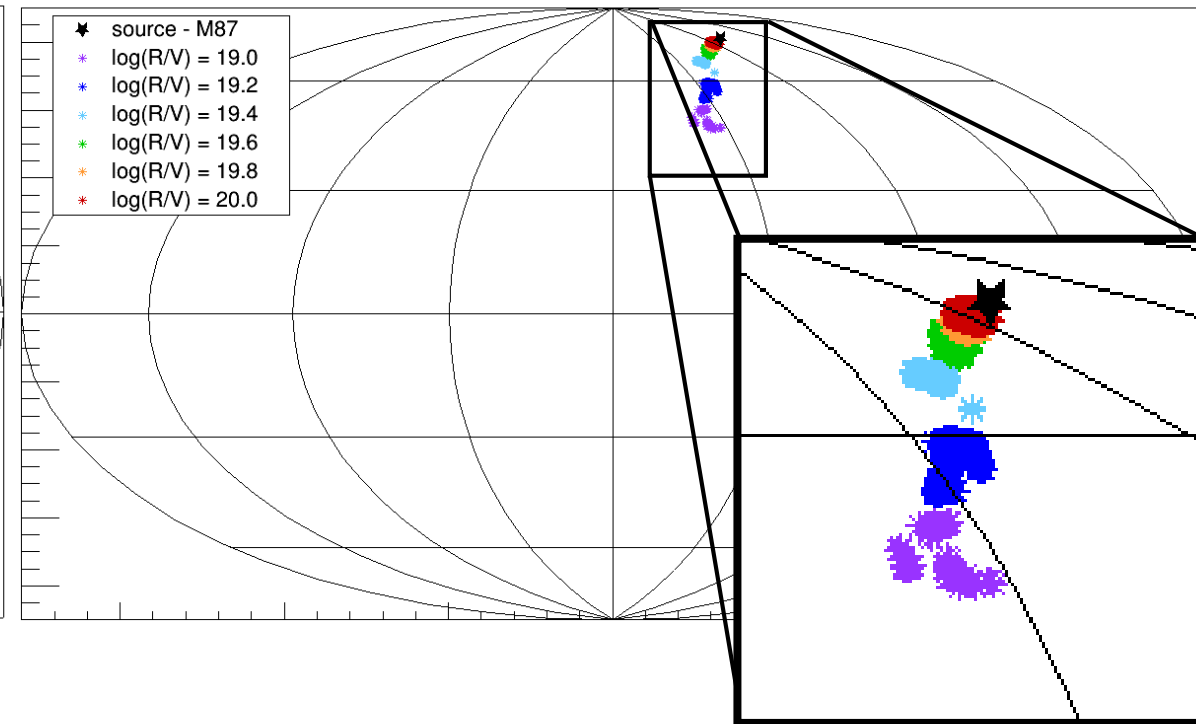
Low rigidity – $10^{18.5}$ V



Deflection of CRs from Candidate Sources



Centaurus A



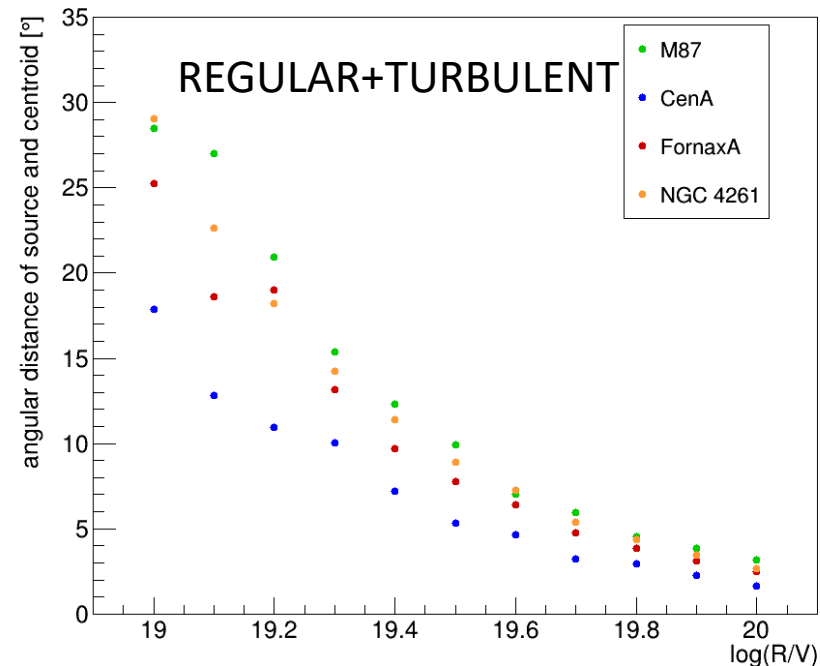
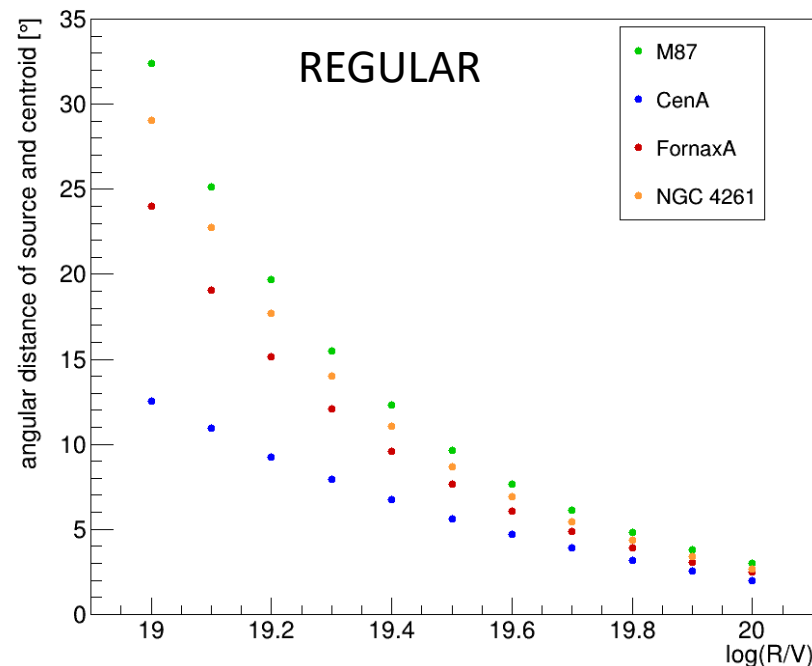
Messier 87

Parametrization of Arrival Regions

- Centroid event = event with minimal sum of angular distances to all other events

$$\sum_{i=1}^N \delta(X_c, X_i)$$

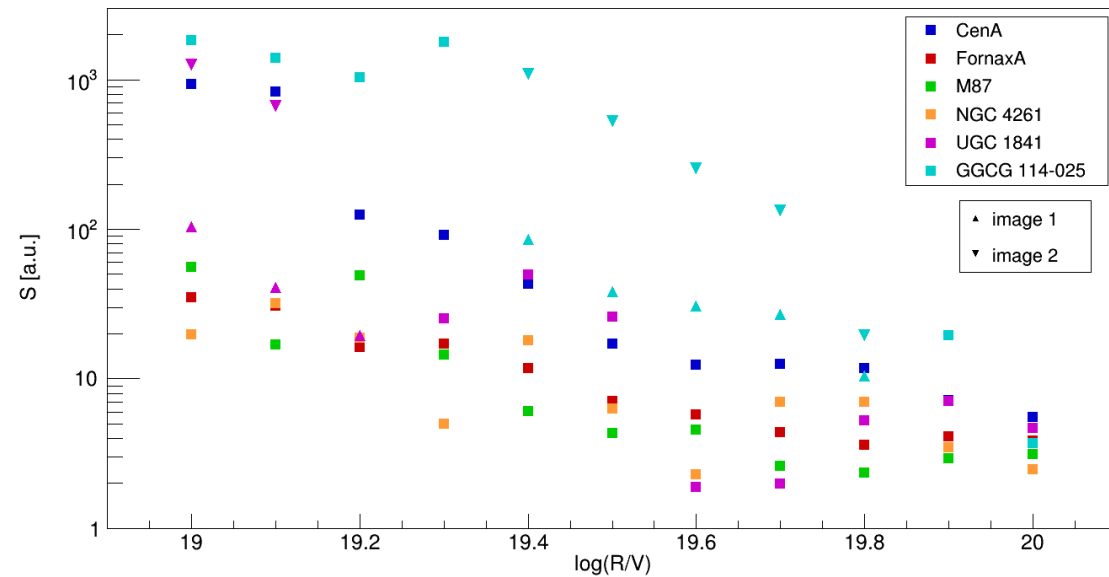
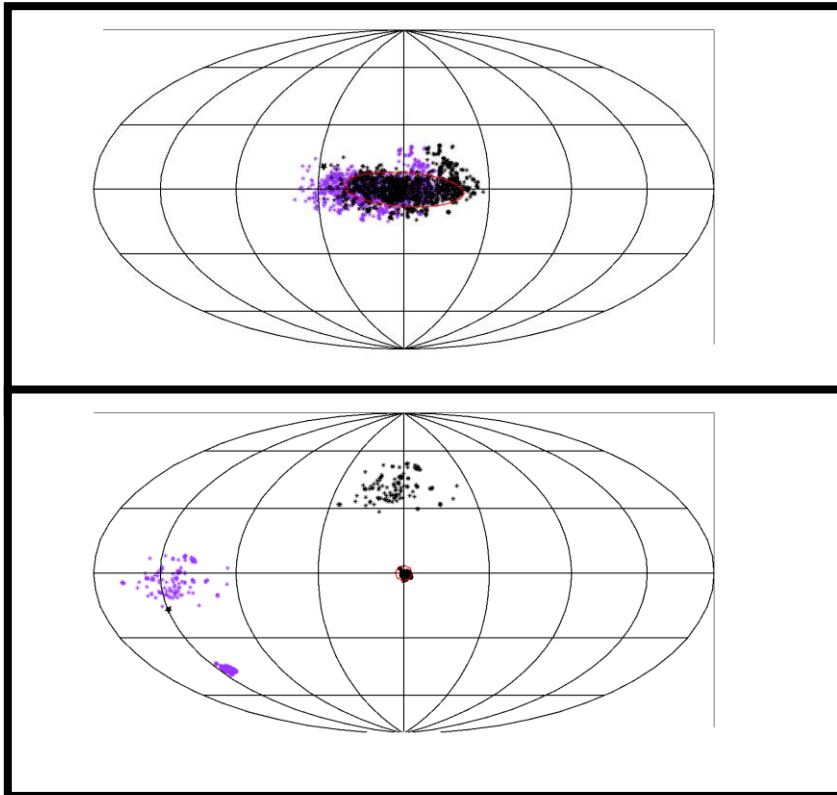
- Regions of arrival directions approximated by an ellipse around a centroid event
- Shifted coordinates so that the centroid is in position (0,0) – Mollweide projection is most planar in the center



Parametrization of Arrival Regions

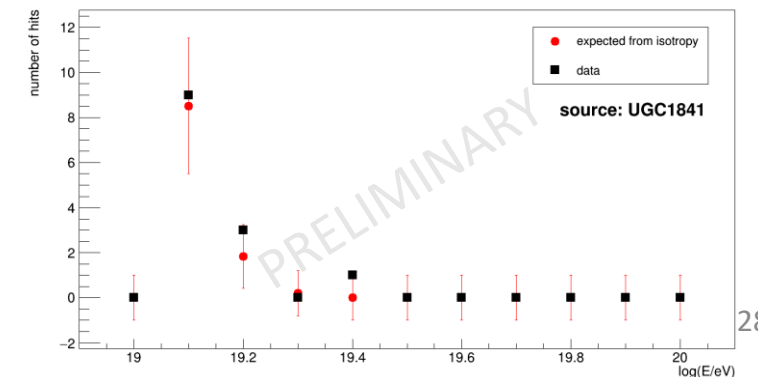
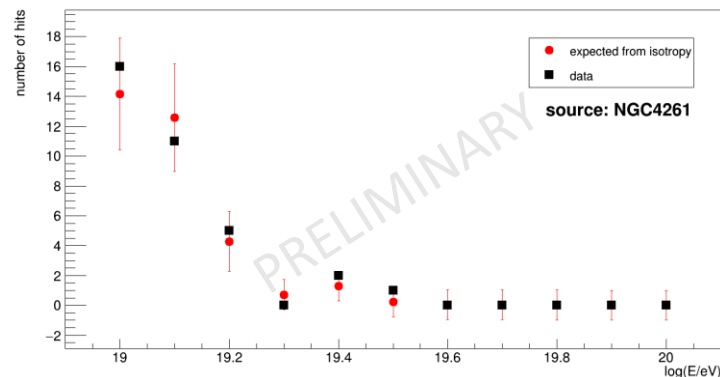
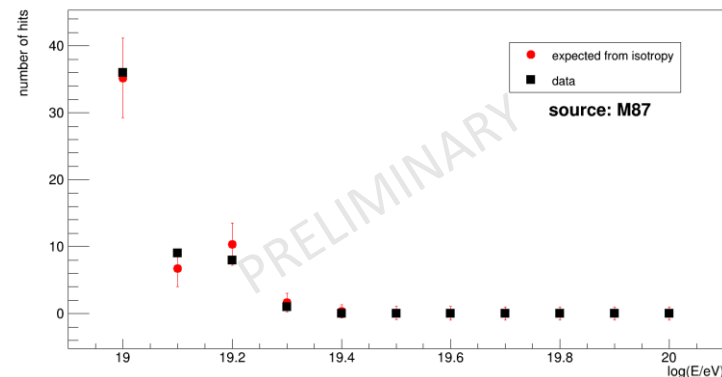
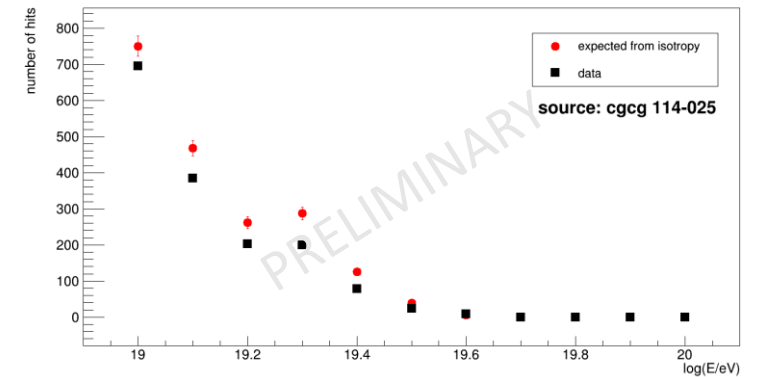
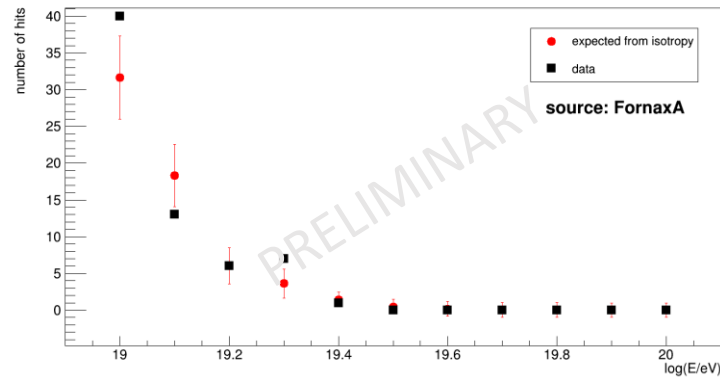
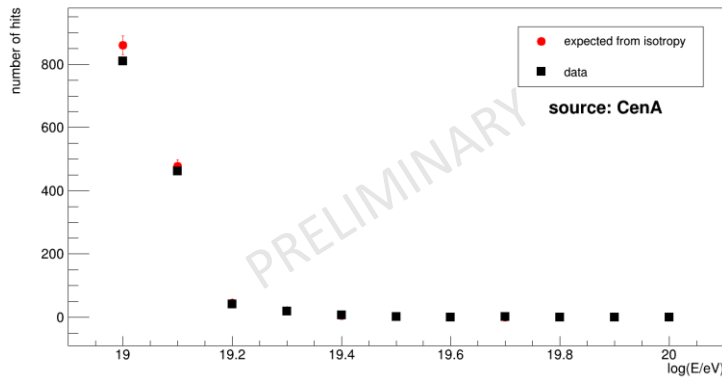
- Minimalization of ellipse area – ellipse needs to contain $\sim 90\%$ of all events

$$S = \pi r_1 r_2 + |N_{in} - 0.9N|/100$$



Search in Data

- Looking for an overall excess of detected events in defined areas for individual sources
- Observed data are also shifted to new coordinates for each source and rigidity region
- For each rigidity area, only events with $E \geq R$ are searched – **NO EXCESS FOUND**



Conclusions and plans

- Composition has a major influence on the amplitude and direction of the observed dipole
- Heavier composition might correspond to a similar direction of the dipole outside the Galaxy as the 2MRS
- Find directions of the injected dipole outside the Galaxy that would end in observed direction of the dipole on Earth

- Galactic magnetic field influences trajectories of cosmic rays even at the highest energies – causes spread of events and shift from the direction of the source
- Deflections strongly depend on source location
- For lower rigidities the deflections can be even tens of degrees
- Proton events are needed to determine sources – heavier nuclei have low R
- Search in observed events for excess in defined areas with composition assumptions

Thank you for your attention!